Scattering by Large Structures with Periodic Surfaces: A Prototype Problem

G.A. KRIEGSMANN
Department of Mathematics
New Jersey Institute of Technology, Newark, NJ 07102
grkrie@ondas.njit.edu
C.L. SCANDRETT
Department of Mathematics
Naval Postgraduate School, Monterey, CA 93942
cscand@boris.math.nps.navy.mil

Abstract

A hybrid method which uses both numerical and asymptotic techniques is described and applied to the scattering of an electromagnetic wave off a large corrugated circular cylinder. The radius of the cylinder is large compared to the wavelength of the incident radiation, but the corrugation height and period are of the same order as the wavelength. This problem is a prototype of a more general situation where the surface of a target is covered with a periodic coating. The method of attack essentially blends boundary layer theory, which describes the local scattering behavior of the surface, and the theory of geometrical optics which gives a global description of the scattering. Although the hybrid method is only developed here for this simple model, its applicability for other targets is clear.

1. Introduction

Although recent advances in computer technology have increased the speed at which engineers and scientists routinely perform large scale scientific computations, there are certain classes of technological problems which can not be efficiently solved by a direct computational approach. These problems typically contain disparate length and/or time scales which make their governing equations ill-conditioned from a numerical point of view. In many cases these disparate scales can be exploited, using asymptotic methods, to yield new approximate equations and boundary conditions which are well suited for numerical methods. This combination of asymptotic and numerical techniques often provides an efficient hybrid method to study the original problem.

An important problem exhibiting these features arises in electromagnetic (and acoustic) scattering theory. There, an incident plane wave of wavelength λ irradiates an electrically (acoustically) large target whose overall size is measured by the length L. By large we mean $L >> \lambda$. Superimposed upon the target is a fine spatial structure which varies on a length scale comparable with λ. This scattering problem poses an extremely difficult boundary value problem from both a computational and analytical point of view. The fine spatial structure suggests employing a fine numerical mesh, but the overall size of the target mitigates against such a numerical attack, regardless of one's computer power. On the other hand, the large overall size of the target suggests an asymptotic method, such as geometrical optics (acoustics), but the fine structure violates the mathematical underpinnings of such an approach. A hybrid method is required to efficiently solve this problem. Unfortunately, such a method does not exist for the general problem just described. To proceed, more information is required about the target shape and the fine structure.

In the case where the fine structure is a homogeneous and isotropic dielectric coating which lies on a PEC surface, considerable progress has been made [1-3]. These authors use a local-planar analysis of the coating to derive a surface impedance that models the layer. This impedance condition is then applied to the PEC surface and the ensuing scattering problem is solved numerically using, for example, a finite difference time-domain technique. This hybrid technique works well for structures whose overall dimension L is not too large compared to λ. On the other hand, this impedance can be used in conjunction with geometrical optics to exploit the size of the structure when $\lambda << L$.

If the fine structure is a periodic coating of dielectric material or the corrugation of a PEC surface, then an analogous procedure can be carried out. Now however, the local analysis is more involved and it requires numerical methods to determine the reflection coefficients for the various Bragg waves that are excited. This kind of

analysis and numerical study have been combined with asymptotic results that exploit the large size of planar structures, such as, corrugated surfaces, gratings, and acoustic arrays of baffled membranes [4-6]. The planar character of the underlying large structure was critical in these analyses.

If the underlying surface which carries the fine periodic structure is not planar, then geometrical optics can be used in conjunction with the local analysis described above. It is intuitive that an incident ray will excite a number of rays, each pointing in the direction of a local Bràgg wave. These scattered rays will each carry an amplitude and a phase governed by the laws of geometrical optics. The initial amplitude and phase on any ray is determined by matching it to the local Bragg wave that generates it. Then the field at any point will be the sum of the fields from each ray. Although the procedure is straightforward in principal, it may become involved if many rays are present.

To illustrate these ideas in a concrete manner, we address here the scattering of a TM wave by a large corrugated circular cylinder whose corrugation is comparable to a wavelength. This "gear-like" structure is shown in Figure 1 where the local period B and the height A are defined. The ordering of these scales is $A \sim B \sim \lambda << L$. The analysis presented here uses the method of matched asymptotic expansions [7] to systematize the ideas in the preceeding paragraph. An inner expansion is developed to analyze the local structure and an outer expansion to exploit the large electrical size of the cylindrical surface.

We now outline the remainder of our paper. Section 2 contains the formulation of the scattering problem in two-dimensions. In Section 3 we define inner variables by scaling the dimensional spatial variables by A. In this scaling the corrugated surface becomes planar and extends to infinity, as $\epsilon \equiv A/L \to 0$, so that the inner problem is identical to the classical scattering problem for a periodic surface. We assume here that an approximate solution to this problem is known (e.g., from a well-conditioned numerical method) and observe that it does not satisfy the proper radiation condition at infinity. Thus, this approximation becomes invalid or nonuniform at large distances.

In Section 4 we introduce a new scaling with respect to L and develop an outer expansion as $\epsilon \to 0$. In this scaling the large corrugated cylinder becomes a smooth cylinder of radius one. The fine structure of the corrugation has been smeared out in this scaling. The geometrical optics method is used to construct the outer solution. We find at each irradiated point on the cylinder the number of rays scattered and their directions. Then we associate with each ray an amplitude and field whose initial values are determined from matching to the inner expansion.

In Section 5 we determine the far field from the outer expansion and specialize the results to determine the backscattered cross-section. This result explicitly shows a multiplicity of specular points and the dependence of these points upon the frequency. Finally in Section 6, we present numerical values for the backscattered cross-section as a function of frequency. These computed values are compared against a full finite difference time-domain simulation for a relatively large corrugated cylinder.

2. Formulation

We take the target to be an electrically large circular cylinder of radius L whose corrugated surface is expressed mathematically by $r = L + Af(\theta)$. Here A is the height of the corrugation measured from the circular surface and $f(\theta)$ is a periodic function whose period B is commensurate with 2π. We also assume that the parameters satisfy the ordering

$$A \sim B \sim \lambda << L \tag{1}$$

where $\lambda = 2\pi c/\omega$ is the wavelength in free space, c is the velocity there, and ω is the frequency of the incident radiation. The structure resembles a gear with many teeth and is shown in Figure 1. Finally, we assume that the structure is a perfect electrical conductor (PEC).

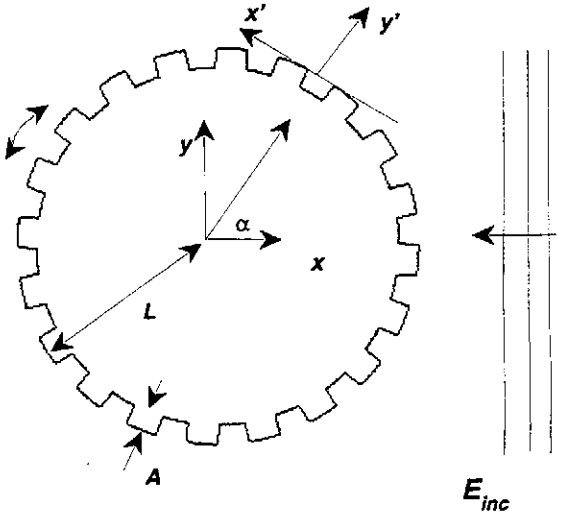

Figure 1 Scattering geometry

A plane time-harmonic TM wave

$$\boldsymbol{E}_{inc} = E_0 e^{-iKx}\hat{z} \equiv u_{inc}\hat{z} \tag{2}$$

impinges upon this structure and scatters from it. The problem then is to determine the scattered field $\boldsymbol{E}_S \equiv u_S\hat{z}$ where the scalar function u_S satisfies the Helmholtz

equation

$$\nabla^2 u_S + K^2 u_S = 0 \tag{3}$$

exterior to the structure and takes on the values

$$u_S = -E_0 e^{-iKx_S}, \qquad x_S \in \partial S \tag{4}$$

where ∂S denotes the surface of the scatterer and $K = 2\pi/\lambda$. In particular, we wish to determine the far-field behavior of $\boldsymbol{E}_S$ or u_S. This is given by

$$u_S \sim D(\theta, K)\frac{e^{iKr}}{\sqrt{Kr}} \tag{5}$$

where D is the differential scattering cross section of the target.

3. The Inner Problem: A Periodic Structure

It is intuitively clear that the surface appears locally as a planar periodic structure. We make this quantitative by introducing the dimensionless inner variables (x', y')

$$x' = \frac{1}{A}\{(y - L\sin\alpha)\cos\alpha - (x - L\cos\alpha)\sin\alpha\} \tag{6}$$

$$y' = \frac{1}{A}\{(y - L\sin\alpha)\sin\alpha + (x - L\cos\alpha)\cos\alpha\} \tag{7}$$

which locally describe the surface near the point $L(\cos\alpha, \sin\alpha)$ on the irradiated portion of the target. The Helmholtz equation becomes, under this transformation

$$\nabla'^2 u_S + k^2 u_S = 0 \tag{8}$$

where $k = KA = O(1)$ is the dimensionless wave number, and the surface is now a periodic function of x' with period $b = B/A$. The incident wave under this transformation becomes

$$u_{inc} = E_0 e^{-iKL\cos\alpha}\, e^{ik(x'\sin\alpha - y'\cos\alpha)} \tag{9}$$

and the boundary condition remains the same

$$u_s = -u_{inc} \tag{10}$$

on the surface. Thus, the local problem is that of an incident plane wave of strength $E_0 e^{-iKL\cos\alpha}$ impinging upon a planar periodic structure (see Figure 2).

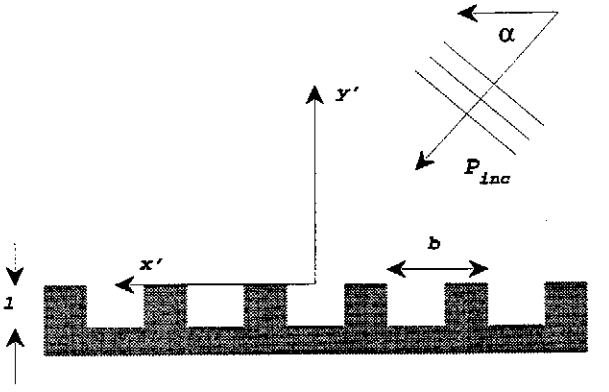

Figure 2: The planar periodic geometry

According to Floquet theory [8] the total field $u = u_{inc} + u_S$ above the periodic structure is given by

$$u = E_0 e^{-iKL\cos\alpha}\, e^{ik(x'\sin\alpha - y'\cos\alpha)} + E_0 \sum_{-\infty}^{\infty} R_n e^{i(\beta_n y' + \gamma_n x')} \tag{11}$$

$$\beta_n = \sqrt{k^2 - \gamma_n^2}\,, \quad \gamma_n = k\sin\alpha + 2n\pi/b \tag{12}$$

where the term $k\sin\alpha$ present in the definition of γ_n is a result of the form of the incident plane wave in the inner coordinates. The reflection coefficients R_n are to be determined.

For a fixed value of k only $M(\alpha) + N(\alpha)$ modes are propagating, namely, $n = -M, \cdots, -2, -1, 0, 1, 2, \cdots, N$. [The propagating modes, or Bragg waves, are those terms in (11) for which the β_n are real and the evanescent modes are those for which they are purely imaginary.] The solution (11,12) represents a finite number of plane waves as $r' \to \infty$ and so does not satisfy the outgoing radiation condition (5). However, the character of these outgoing waves can be used to construct a radiation boundary operator which can be numerically implemented along with a finite difference or finite element approximation of the boundary value problem (8,9,10) to construct an accurate approximation of this inner solution [9,10]. These numerical results can then be used to approximately determine the reflection coefficients R_n.

Finally, as noted above, the structure of the scattered field given by the second term in (11) does not behave as an outgoing cylindrical wave in the far field, and so a new expansion for u must be determined in this region.

4. The Outer Solution

To initiate the study of the outer expansion, outer variables scaled on the radius L must be introduced.

They are $(X,Y) = \frac{1}{L}(x,y)$. Then, the Helmholtz equation becomes

$$\left\{ \frac{\partial^2}{\partial X^2} + \frac{\partial^2}{\partial Y^2} \right\} u + \frac{k^2}{\epsilon^2} u = 0 \tag{13}$$

where $\epsilon = A/L << 1$. In this scaling all the fine structure of the corrugated surface is smeared out along the circle $R = \sqrt{X^2+Y^2} = 1$, so that the solution of (13) is required away from this surface. Moreover, the presence of the the ϵ in (13) suggests a high frequency or geometrical optics approach.

Accordingly we seek an asymptotic approximation to the solution of (13) of the form

$$u = E_0 e^{-ikX/\epsilon} + E_0 \sum A_n e^{i(k/\epsilon)\Psi_n} \tag{14}$$

where each phase function Ψ_n satisfies the eiconal equation

$$|\nabla \Psi|^2 = 1 \tag{15}$$

and each amplitude satisfies the transport equation

$$2\nabla A \cdot \nabla \Psi + A \nabla^2 \Psi = 0. \tag{16}$$

The form of this solution is suggested by the structure of the inner solution; each term in the sum corresponds to a local Bragg wave launched from a point on the surface in the direction of (X,Y). Moreover, the number of rays at a given point depends upon α.

Consider an incident ray striking the surface $R = 1$ at the point $(\cos\alpha, \sin\alpha)$. A family of $M(\alpha) + N(\alpha)$ scattered rays emerge from this point, the *nth* being given by

$$(X,Y) = (\cos\alpha, \sin\alpha) + \tau(p_n(\alpha), q_n(\alpha)) \tag{17}$$

where (p_n, q_n) is a unit vector along the line. The corresponding phase function Ψ_n along this ray is given by

$$\Psi_n = \Psi_n^0(\alpha) + \tau \tag{18}$$

where Ψ_n^0 is a constant which will be determined shortly. Similarly, the amplitude which satisfies (16) is

$$A_n = \frac{A_n^0(\alpha)}{\sqrt{J(\tau,\alpha)}} \tag{19}$$

where the Jacobian J is defined by

$$J = X_\tau Y_\alpha - X_\alpha Y_\tau. \tag{20}$$

Here the subscripts denote partial differentiation.

In the Appendix we show by matching the field associated with the *nth* ray, as $\tau \to 0$, with the inner solution, as $x'^2 + y'^2 \to \infty$, that

$$\Psi_n^0(\alpha) = 0, \qquad A_n^0(\alpha) = R_n \sqrt{J(0,\alpha)}, \tag{21}$$

and

$$\begin{aligned} p_n &= B_n \cos\alpha - G_n \sin\alpha \\ q_n &= B_n \sin\alpha + G_n \cos\alpha \end{aligned} \tag{22}$$

where $B_n = \beta_n/k$ and $G_n = \gamma_n/k$. The Jacobian can now be computed using its definition (20) and (22). Inserting this expression into (19) and using the initial data for A_n given in (21), the amplitude becomes

$$A_n = \frac{R_n B_n}{\sqrt{B_n^2 + \tau(B_n + \cos\alpha)}}. \tag{23}$$

The field associated with this ray is then given by (18),(21), and (23), i.e.

$$u_n = E_0 \frac{R_n B_n}{\sqrt{B_n^2 + \tau(B_n + \cos\alpha)}} e^{i\tau/\epsilon}. \tag{24}$$

The field at any point (X,Y) is determined by finding the totality of rays passing through it and by summing up the fields associated with each ray. This may be a formidable task, as the rays come from different points $(\cos\alpha, \sin\alpha)$ on the illuminated portion of the target. We shall not pursue this point further here.

5. The Far Field

The process of determining those rays which pass through a given point (X,Y) simplifies considerably in the far field where $R >> 1$. Focusing on the n^{th} ray emanating form the point $(\cos\alpha, \sin\alpha)$, an application of the law of cosines to (17) gives

$$\tau \sim R - B_n(\alpha), \qquad \Psi_n = R - B_n(\alpha) \tag{25}$$

and using the first part of this in (10c) yields

$$A_n = \frac{R_n B_n}{\sqrt{B_n + \cos\alpha}} \frac{1}{\sqrt{R}}. \tag{26}$$

Setting $X = R\cos\theta$ and $Y = R\sin\theta$ into (17) and using (25), a simple relationship is obtained for θ as a function of α. It is

$$\theta = \alpha + \phi_n(\alpha) \tag{27}$$

where $\cos\phi = \beta_n/k$. Omitting a lengthy trigonometric calculation, this expression can be rewritten as

$$\sin\alpha = \frac{-\eta}{2} \left\{ 1 - \sqrt{\frac{4}{\eta^2}\sin^2(\theta/2) - \tan^2(\theta/2)} \right\} \tag{28}$$

where $\eta = 2n\pi/kb$. The roots $\alpha(\theta)$ of (27) are now given by the roots of (28). Clearly, (28) can be inverted as long as the right hand side of this expression is less than one. One case is worth noting explicitly here: for a fixed value of θ and $n = 0$, (28) gives $\sin\alpha = \sin(\theta/2)$ or $\alpha = \theta/2$. This is the specular result for a smooth PEC cylinder.

To further develop these ideas fix a value of k. Then for a given value of θ (28) will have a solution for at most a finite number of n. Let $\alpha_\nu(\theta)$ be one such solution. Then the far field result is found by combining (25,26,27,28), the definition of B_n, and (14). It is

$$u(X,Y) = E_0 e^{-ikX/\epsilon}$$

$$+ E_0 \left[\sum_\nu \frac{R_\nu \cos\phi_\nu e^{-i(k/\epsilon)\cos\phi_\nu}}{\sqrt{\cos\alpha_\nu + \cos\phi_\nu}} \right] \frac{e^{i(k/\epsilon)R}}{\sqrt{R}} \qquad (29)$$

where the sum is over the rays passing through (X,Y) and $\beta_\nu = \theta - \alpha_\nu(\theta)$.

Finally we observe that the above results simplify even more when $\theta = 0$, i.e., in the backscattered direction. Then, (28) simplifies to

$$\sin\alpha = -n\pi/kb \qquad (30)$$

which again has a solution for at most a finite number of n. For each of these roots $\phi_\nu = -\alpha_\nu$. Consequently, the total far field in the backscatter direction is given by (29) as

$$u(X,Y) = E_0 e^{-ikX/\epsilon} + S(0,k)\frac{e^{i(k/\epsilon)R}}{\sqrt{R}} \qquad (31)$$

$$S(0,k) = \frac{E_0}{\sqrt{2}} \sum_\nu R_\nu \sqrt{\cos\alpha_\nu} e^{-i(k/\epsilon)\cos\alpha_\nu} \qquad (32)$$

where the sum is over the back scattered rays. Expressing R in terms of r and comparing the scattered field in (31) with (5) gives

$$D(0,K) = \sqrt{k/\epsilon}\, S(0,k). \qquad (33)$$

6. Numerical Examples

In this section the backscattered cross section $D(0,k)$ will be determined from (31,32,33) for the range of frequencies corresponding to $0 < kb < 2\pi$. This result will be compared against a time-domain finite difference approximation of the scattering problem for the target shown in Figure 1.

Since the target is symmetric, we need only consider $0 < \alpha < \pi/2$. Thus, (30) implies that only negative values of n need be considered. When $0 < kb < \pi$ equation (30) has only one real root. This occurs for $n = 0$ and $\alpha = 0$. The backscattered cross section $D(0,k)$ for this range of k is

$$D(0,k) = \sqrt{\frac{k}{2\epsilon}} R_0(0) e^{-ik/\epsilon}, \quad 0 < kb < \pi. \qquad (34)$$

When kb is increased to lie in the interval $\pi < kb < 2\pi$, then (30) admits another solution $n = -1$ and $\alpha = \alpha_{-1} = \sin^{-1}\pi/kb$. The expression for the backscattered cross section is now

$$D(0,k) = \sqrt{\frac{k}{2\epsilon}} \left[R_0(0) e^{-ik/\epsilon} \right.$$

$$\left. + 2R_{-1}(\alpha_{-1})\sqrt{\cos(\alpha_{-1})}\, e^{-i(k/\epsilon)\cos(\alpha_{-1})} \right] \qquad (35)$$

where the factor of two arising in the second term comes from the symmetry of the problem. For $2\pi < kb < 3\pi$ (30) admits another new root which adds another term into (35); this process goes on for increasing values of kb.

The numerical evaluation of $D(0,k)$ requires the reflection coefficients $R_0(0)$ and $R_{-1}(\alpha_{-1})$ as functions of k in the interval $0 < kb < 2\pi$.This can be done using the finite difference scheme reported in Reference 10 or the finite element method reported in Reference 11.

We have used a finite difference time-domain technique and a radiating mode extinction algorithm in the far-field to determine the reflection coefficients for the inner "waveguide" problem. A standard finite difference time-domain methodology for the full scattering from the "gear" was used but with the much simpler second order two-dimensional radiation condition. Care was taken to ensure that a minimum of 20 nodes per wavelength (determined by the incident frequency) was used, and that phase differences due to differing iteration stopping times for the waveguide problem were scaled out. In each case a stopping criterion involving variations of the scattered wave amplitude was used to determine convergence of the numerical schemes.

The actual physical parameters of the "gear" scattering problem (scaled by the height of the corrugations A) are: $L = 100/\pi^2 \approx 10$, $B = 10/\pi \approx 3$, width of slot $= B/2$, and there are 20 equally spaced slots in the "gear". The mesh for the "gear" problem had varying Δt, but the spatial grid was fixed at $\Delta\theta = \pi/400$ and $\Delta r = 1/12$. The physical parameters for the waveguide problem were made to be commensurate with those taken from the gear scattering. In particular, $\Delta y' = \Delta r$ and $\Delta x' = L\Delta\theta = 1/4\pi$.

The results of these calculations are shown in Figure 3 where the results of the present hybrid theory (34,35) are given by the solid curve and where the results of the full numerical simulation of the gear scattering are given by the dotted curve. The agreement is excellent, showing that the hybrid method predicts an accurate result. Tha major discrepancies occur at $kb = n\pi$ where new Bragg modes are initiated in the inner problem. The other minor errors are caused by the fact that (34,35) are asymptotic results as $\epsilon = A/L \to 0$ and in the present example $\epsilon = 0.1$.

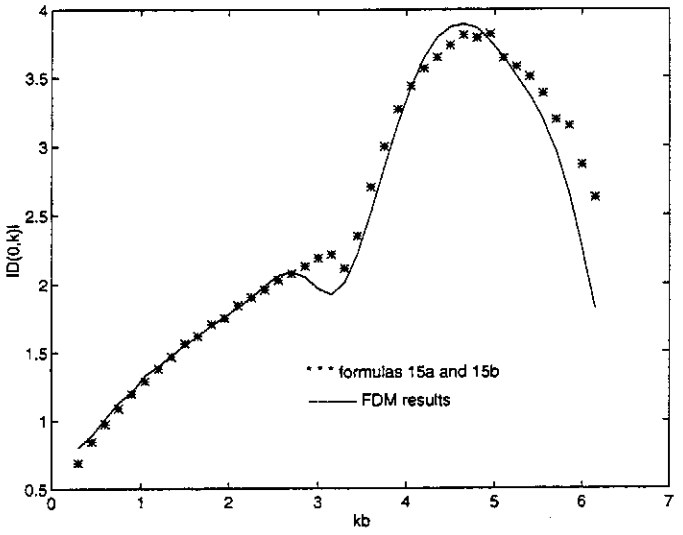

Figure 3: Comparison of backscattered data

References

1. T.B.A. Senior and J. L. Volakis, **Radio Science**, Vol. 22, 1987, pp. 1261-1272.

2. D. J. Hoppe and Y. Rahmat-Samii, **IEEE Trans. Antennas Propagation**, Vol. 40, 1992, pp. 1513-1523.

3. T.B.A. Senior and J. L .Volakis, **IEEE Trans. Antennas Propagation**, Vol. 37, 1989, pp. 744-750.

4. G. A. Kriegsmann, **J. Acous. Soc. Am.**, Vol. 88, 1990, pp. 492-495.

5. G. A. Kriegsmann, "A Hybrid Method for Large Gratings", Proceedings of the 2nd Congress on Applied Mathematics, Oviedo Spain, 1991.

6. G. A. Kriegsmann and C. L. Scandrett, **J. Acous. Soc. Am.**, Vol. 93, 1993, pp. 3043-3048.

7. J. D. Cole, *Perturbation Methods in Applied Mathematics* (Blaisdell, Waltham, MA, 1968).

8. C. Wilcox, *Scattering Theory for Diffraction Gratings*, Applied Math. Series, No. 48 (Springer-Verlag, New York, 1984).

9. C. L. Scandrett and G. A. Kriegsmann, **J. Comp. Phys.**, Vol. 111, 1993, pp. 282-290.

10. B. J. McCarten and G. A. Kriegsmann, **J. Electromag. Waves and Appl.**, Vol. 9, N0.5/6, 1995, pp.615-643.

Appendix

According to the principal of matching [7], the inner and outer expansions must agree in a small layer where both expansions are valid. In this layer one equates the inner expansion (11) for $\sqrt{x'^2 + y'^2} >> 1$ with the outer expansion (14) as $\tau \to 0$. This can be done efficiently by expressing (11) in terms of the outer variables and comparing the result with (14). Upon inserting the outer variables into the right hand side of (6, 7) and using this new expression in (11), we obtain

$$u_S = \sum_{-\infty}^{\infty} R_n e^{i(k/\epsilon)[p_n(X-X_0)+q_n(Y-Y_0)]}$$

where p_n and q_n are defined in (22). Since p_n and g_n have components that are proportional to β_n, and β_n is purely imaginary for $n > n(\alpha)$ and for $n < -M(\alpha)$, the sum need only run from $-M$ to N. This just states that the evanescent modes are essentially zero in this matching region. Comparing this expression with (14, 17, 18, 19, 20) as $\tau \to 0$ yields (21, 22, 23, 24).

Acknowledgement

G. A. Kriegsmann was supported by the Air Force Office of Scientific Research, Grant # AFOSR 91-0252.